

Direction of Arrival (DOA) Estimation for Smart Antennas in Weather Impacted Environments

Bongani P. Nxumalo* and Tom Walingo

Abstract—Direction of arrival estimation (DOA) is critical in antenna design for emphasizing the desired signal and minimizing interference. The scarcity of radio spectrum has fuelled the migration of communication networks to higher frequencies. This has resulted in radio propagation challenges due to the adverse environmental elements otherwise unexperienced at lower frequencies. In rainfall-impacted environments, DOA estimation is greatly affected by signal attenuation and scattering at the higher frequencies. Therefore, new DOA algorithms cognisant of these factors need to be developed and the performance of the existing algorithms quantified. This work investigates the performance of the Conventional Minimum Variance Distortion-less Look (MVDL), Subspace DOA Estimation Methods of Multiple Signal Classification (MUSIC), and the developed estimation algorithm on a weather impacted wireless channel, Advanced-MUSIC (A-MUSIC). The results show performance degradation in a rainfall impacted communication network with the developed algorithm showing better performance degradation.

1. INTRODUCTION

Smart antenna systems merge antenna arrays with intelligent digital signal processing ability in order to transmit and receive in a versatile and spatially delicate way. Different users are served with narrow beam radiation patterns, thus reducing multipath and co-channel interference and enhancing frequency reuse. They determine spatial signal signature, direction of arrival (DOA) or angle of arrival (AOA), and use it to estimate the beamforming vectors, to track and identify the antenna beam. Thus, the most critical parts of smart antennas are DOA estimation and beamforming [1]. The accurate estimation of the DOA of all signals transmitted to the adaptive array antenna enables the maximization of its performance with respect to recovering the required transmitted signal and suppressing any presence of interfering signals. The beamforming technique also ensures less interference to the system, thus increasing the overall system performance. The development of efficient DOA algorithms is critical for the performance of the communication networks. Traditionally, the developed DOA algorithms are popularly classified into two main categories: the conventional Beamforming [2, 3], e.g., Bartlett and Capon (Minimum Variance Distortionless Response (MVDR)) and the Subspace DOA Estimation Methods such as the Multiple Signal Classification (MUSIC) and Estimation of Signal Parameters via Rotational Invariance Techniques (ESPRIT). In the conventional MVDR technique, the Bartlett algorithm, Fourier based spectral analytical techniques are applied to the spatio-temporarily sampled data of mostly a single signal. It was extended to multiple signals by Capon to contain signal contributions from the desired angle as well as the undesired angle as the Minimum Variance Algorithm [4]. The Bartlett algorithm maximises the power of beamforming output for a given input signal whereas the Capon algorithm attempts to minimize the power contributed by noise and any

Received 10 May 2019, Accepted 19 July 2019, Scheduled 10 September 2019

* Corresponding author: Bongani Prudence Nxumalo (217080449@stu.ukzn.ac.za).

The authors are with the Discipline of Electrical, Electronic and Computer Engineering, University of KwaZulu-Natal, Durban 4041, Republic of South Africa.

signals coming from other direction than desired. Both methods involve spectrum evaluation followed by finding the local maxima that give the estimated DOA. However, these methods are highly dependent on physical antenna aperture array size resulting in poor resolution and accuracy [2, 4]. In addition, they do not exploit the structure of the narrowband input data model of the measurements.

Subspace techniques conduct characteristic decomposition of the covariance matrix for any array output data, resulting in a signal subspace orthogonal with to noise subspace corresponding to the signal components. Estimation of DOA is performed from one of these subspaces, assuming that noise in each channel is highly uncorrelated. The popularity of the MUSIC algorithm [5] is due to its generality. It is applicable to arrays of arbitrary but known configuration and response, used to estimate multiple parameters per source. MUSIC algorithm has the ability to simultaneously measure multiple signals with high precision and resolution among others. However, the conventional MUSIC algorithm requires a priori knowledge of the second-order spatial statistics of the background noise and interference field. It also involves a computationally demanding spectral search over the angle, therefore, expensive in implementation. The ESPRIT [6] is a computationally efficient and robust subspace method of DOA estimation. It uses two identical matched array pairs aiding it in reducing complexity. Although ESPRIT alleviates the computational complexity of MUSIC algorithm, it is more prone to errors [10]. Other algorithms also exist for DOA estimation. The development and performance evaluation of these algorithms and their variants has been exhaustively done for the legacy communication network environments [4, 7–10] and need not be reemphasised.

The increasing demand on mobile broadband services has led to the scarcity of radio spectrum due to spectrum exhaustion [11]. This has led to migration to higher frequency millimetre-wave (mmW) bands, which range from 30 GHz to 300 GHz, for mmW communication with additional large bandwidths. Apart from the merits of expanded bandwidth and high frequency reuse packing due to shorter wavelengths, mmW communication, possess its own challenges including large path loss suffered by mmW signals, and the effect of the weather effectors to signals in this band. Rainfall is a common weather phenomenon that affects signal transmission at this band. In link budget planning and design at lower frequencies, rainfall is considered as a fixed propagation attenuation [12]. The transmitted signal suffers from absorption from the rain causing signal attenuation. In mmW systems, the wavelengths of the signals are comparable to the raindrop size from 0.1 mm to 10 mm [13]. Hence, apart from attenuation, the signals undergo scattering when being transmitted through rain leading to both amplitude attenuation and phase fluctuation [14]. Rain attenuation and scattering are a function of the rain rate, polarization, physical size of drops and operating frequency [15, 16]. Rainfall attenuation, frequency attenuation, and phase distortion affect the received signal. For these mmW systems, DOA algorithms that do not consider the effect of the weather are not realistic. This work is among the first that investigates the performance of the DOA algorithms in a rainfall-impacted network and develops a hybrid algorithm to combat the rainfall effects in DOA estimation. A realistic Markovian rainfall channel model is used to accurately capture the rainfall variations in three cases; widespread, shower and thunderstorm rain events.

The rest of the paper is organized as follows. In Section 2, the system model is presented. Section 3, represents the weather channel parameter modelling. The proposed method of efficiently estimating the DOA and other conventional and subspace DOA estimation algorithms are presented in Section 4. In Section 5, the performance measures and overall performance evaluation algorithm is done while simulation results and discussion are presented in Section 6. The paper concludes in Section 7.

Notation: The bold upper and lower-case letters represent the matrices and column vectors, respectively. I is an identity matrix. The following superscripts $(\cdot)^*$, $(\cdot)^H$, $(\cdot)^{-1}$ and $(\cdot)^T$ represent optimality, Hermitian, inverse and transpose operators, respectively and $E(\cdot)$ is the mathematical expectation, d is the spacing difference between array elements, c is the speed of light and λ is the wavelength.

2. SYSTEM MODEL

The DOA algorithms estimate the angle of arrival of all incoming signals. In Figure 1 a uniform linear array (ULA) of N equally spaced sensors is shown. A source transmits signals $s(t)$ that after passing through a weather-impacted environment arrives at the antenna at an angle θ . The signals $x(t)$ induced

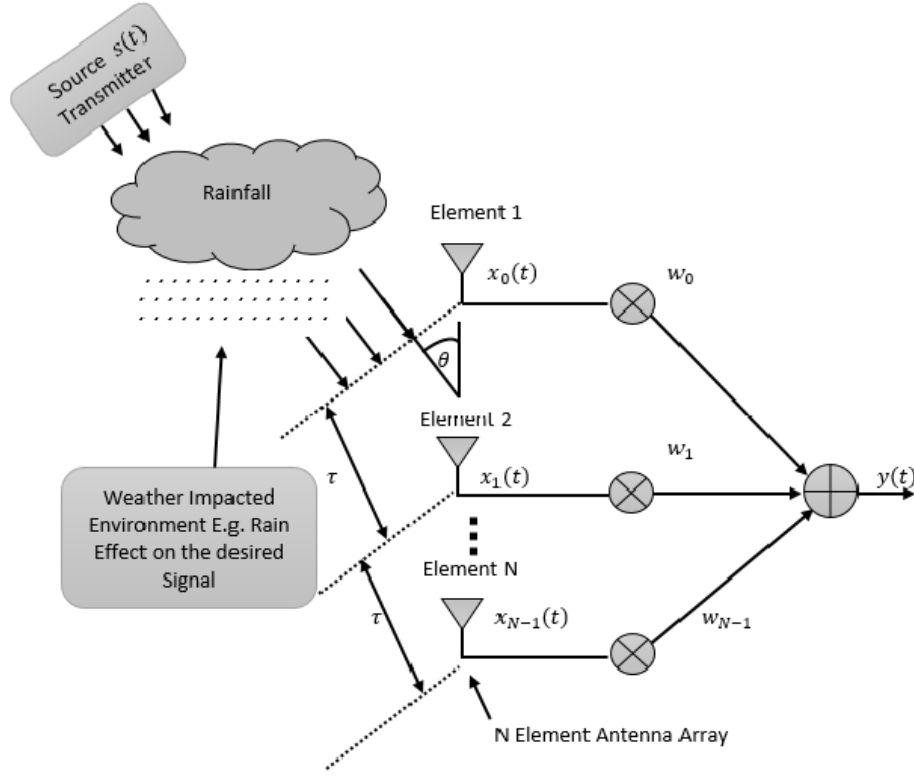


Figure 1. System model.

on the antenna arrays are multiplied by adjustable complex weights w and then combined to form the system output $y(t)$. The processor receives array signals, system output, and direction of the desired signal as additional information. In our model, for a wavefront narrow band signal $s_i(t)$, the received signal $x_i(t)$ at antenna element, $i = 1, 2, \dots, N$, is given by

$$x_i(t) = \sum_{i=1}^N \alpha_i s_i(t) a_i(\theta_i + \Delta\theta_i) + v_i(t), \tag{1}$$

where α_i is the rainfall attenuation, θ_i the angle of arrival, $\Delta\theta_i$ the rainfall angle deviation, and v_i the measured noise at antenna i . The response function of the array element i to the signal source $a_i(\hat{\theta}_i)$ is

$$a_i(\hat{\theta}_i) = \exp \left[-j(i-1) \frac{2\pi d \sin \hat{\theta}_i}{\lambda} \right], \tag{2}$$

where λ is the wavelength, and d is the spacing difference between array elements. The total received signal vector $X(t)$ is expressed as:

$$X(t) = A(\hat{\theta})\tilde{S}(t) + V(t), \tag{3}$$

where

$$\begin{aligned} X(t) &= [x_1(t), x_2(t), \dots, x_N(t)]^T, \\ A(\hat{\theta}) &= [a_1(\hat{\theta}_1), a_2(\hat{\theta}_2), \dots, a_N(\hat{\theta}_N)]^T, \\ \tilde{S}(t) &= [\tilde{s}_1(t), \tilde{s}_2(t), \dots, \tilde{s}_N(t)]^T, \\ V(t) &= [v_1(t), v_2(t), \dots, v_N(t)]^T. \end{aligned} \tag{4}$$

In Equation (4), $\tilde{s}_i(t) = \alpha_i s_i(t)$ and $\hat{\theta}_i = \theta_i + \Delta\theta_i$. The modelling and investigation of the rainfall attenuation α_i and angle deviation $\Delta\theta_i$ due to the weather impacted rainfall channel are done in the next section.

3. WEATHER CHANNEL PARAMETER MODELLING

3.1. Rainfall Modeling

The magnitude of attenuation experienced by signals depends on the rain intensity. Based on its intensity, a rain event may be classified as drizzle (D), widespread (W), shower (S), or thunderstorm (T). The rainfall is modelled by four or fewer states of a Markov Chain, R , given by

$$R = \{D, W, S, T\}, \tag{5}$$

Table 1 presents the rain event intensities.

Table 1. Rain rates categories.

Description	Rain Rate (r)	Steady State (π_n)
Drizzle	1–5	π_D
Widespread	5–10	π_W
Shower	10–40	π_S
Thunderstorm	> 40	π_T

Practical rainfall, widespread, shower and thunderstorm events consist of a mix of the different rain events [17]. This work utilizes Markov models developed from actual rain data to model practical rain events, with the transition diagram and state transition probabilities as given bellow:

- i) Widespread rainfall: Consists of drizzle and widespread events. The transition diagram shown in Figure 2, with the transitional probabilities, $P_{i,j}^W$, form states i to j , with $i, j \in R$, given by Equation (6)

$$P_{i,j}^W = \begin{bmatrix} P_{DD} & P_{DW} \\ P_{WD} & P_{WW} \end{bmatrix}, \tag{6}$$

where P_{DW} is the probability of transition from drizzle to widespread, P_{WD} the probability of transition from widespread to drizzle, P_{DD} the probability of no transition from drizzle, and P_{WW} the probability of no transition from widespread.

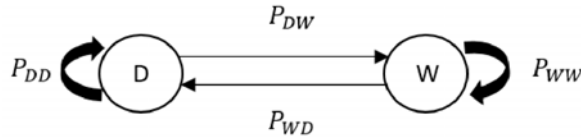


Figure 2. Widespread rainfall.

- ii) Shower rainfall consists of drizzle, widespread and shower events. The transition diagram shown in Figure 3, with the transitional probabilities, $P_{i,j}^S$, form states i to j , with $i, j \in R$, given by Equation (7)

$$P_{i,j}^S = \begin{bmatrix} P_{DD} & P_{DW} & P_{DS} \\ P_{WD} & P_{WW} & P_{WS} \\ P_{SD} & P_{SW} & P_{SS} \end{bmatrix}, \tag{7}$$

where P_{DS} is the transition probability from drizzle to shower, P_{WS} the transition probability from widespread to shower, P_{SD} the transition probability from shower to drizzle, P_{SW} the transition probability from shower to widespread, and P_{SS} the no transition probability from shower.

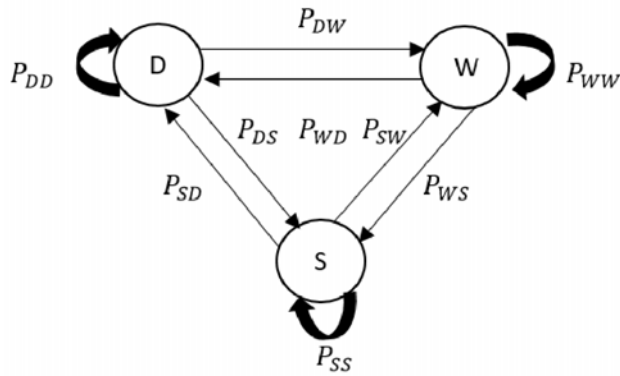


Figure 3. Shower rainfall.

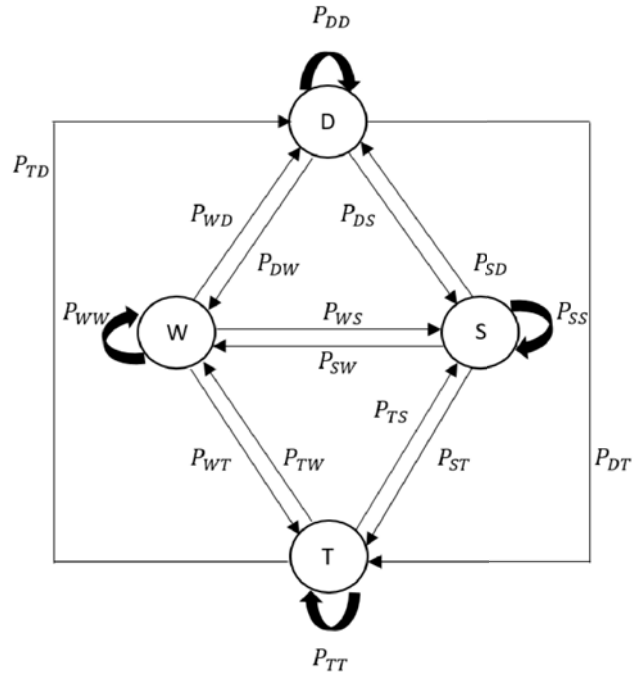


Figure 4. Thunderstorm rainfall.

iii) Thunderstorm rainfall consists of drizzle, widespread, shower and thunderstorm events. The transition diagram shown in Figure 4, with the transitional probabilities, $P_{i,j}^T$, form states i to j , with $i, j \in R$, given by Equation (8)

$$P_{i,j}^T = \begin{bmatrix} P_{DD} & P_{DW} & P_{DS} & P_{DT} \\ P_{WD} & P_{WW} & P_{WS} & P_{WT} \\ P_{SD} & P_{SW} & P_{SS} & P_{ST} \\ P_{TD} & P_{TW} & P_{TS} & P_{TT} \end{bmatrix}, \tag{8}$$

where P_{DT} is the probability of transition from drizzle to thunderstorm, P_{WT} the probability of transition from widespread to thunderstorm, P_{ST} the probability of transition from shower to thunderstorm, P_{TD} the probability of transition from thunderstorm to drizzle, P_{TW} the probability of transition from thunderstorm to widespread, P_{TS} the probability of transition from thunderstorm to shower, and P_{TT} the no transition probability from thunderstorm. The transitional probabilities used are practically obtained from [17]. The steady state probability of an event n , $\pi_n = \{\pi_D, \pi_W, \pi_S, \pi_T\}$, is solved by the standard Markov chain solution methods. The expected rate for a rainfall occurrence is derived from the probabilities as

$$E[r] = \sum_n r_n \pi_n, \tag{9}$$

where r_n is the median rain event, and π_n is the steady state probability of the n th state of the Markov model. The actual rain rate r is computed from a lognormal distribution with the given mean [17–19].

3.2. Attenuation Model

We consider a radio propagation environment where the signal is affected by attenuation due to the weather-impacted factors. The total attenuation A_T is given by

$$A_T = \alpha_i + L_{fs}, \tag{10}$$

where α_i is the rain attenuation. The ITU rainfall model [20] is used for attenuation as

$$\alpha_i = kr^a, \quad (11)$$

where r is the rain rate in mm/hr of Section 3.1. The constant parameter k and exponent a depend on the frequency f (GHz), the polarization state, and the elevation angle of the signal path. Free space loss attenuation, L_{fs} , is given by

$$L_{fs} = 20 * \log_{10} \frac{4\pi d}{\lambda}, \quad (12)$$

where λ is the signal wavelength in metres, and d is the distance from the transmitter.

3.3. Angle Deviation Model

The weather related factors result in the delay and scattering of the transmitted signal as well as phase angle and angle deviation change. The angle deviation, $\Delta\theta_i$, is modelled as a normal distributed random variable with a mean μ_θ bounded as follows

$$\Delta\theta_{\min} \leq \Delta\theta_i \leq \Delta\theta_{\max}, \quad (13)$$

where $\Delta\theta_{\min}$ and $\Delta\theta_{\max}$ are the minimum and maximum angle deviations, respectively. The mean μ_θ is derived from the normalised rain rate

$$\mu_\theta = \frac{r}{r_{\max}}, \quad (14)$$

and r_{\max} is the maximum rain rate. The assumption is reasonable as the heavier the rain, the more the scattering. Though the weather elements affect the mean and the standard deviation, we keep the standard deviation constant.

4. DOA ESTIMATION ALGORITHMS

4.1. MVDR Algorithm

The MVDR algorithm minimizes the output power and constrains the gain of the direction of desired signal to unity [21] as follows,

$$\min E\{|y_n(t)|^2\} = \min\{w^H \sigma(x, x)w\}, \quad (15)$$

subject to $w \cdot a(\hat{\theta}) = 1$ where

$$y_n(t) = w^H \sigma(x, x)w, \quad (16)$$

is the output of the array system, w the weight vector, H the Hermitian matrix, $a(\hat{\theta})$ the steering vector, and $\sigma(x, x)$ covariance matrix of the received signal x . The covariance matrix $\sigma(x, x)$ is given by

$$\sigma(x, x) = \frac{1}{N} \sum_{i=1}^N xx^H, \quad (17)$$

where N is the number of elements. From the block diagram of Figure 1, the signal vector $x(t)$ defined at different angles $\hat{\theta}_i$ induced on the antenna arrays is multiplied by weight vectors w and then combined to form the system output $y(t)$. The weighted vector w is obtained by using Lagrange multiplier in Eq. (15) as

$$w = \frac{(\sigma(x, x))^{-1}a(\hat{\theta})}{a^H(\hat{\theta})(\sigma(x, x))^{-1}a(\hat{\theta})}. \quad (18)$$

Thus, MVDR computed as a Capon's output power spectrum is given by

$$P_{MVDR}(\hat{\theta}) = \frac{1}{a^H(\hat{\theta})(\sigma(x, x))^{-1}a(\hat{\theta})}. \quad (19)$$

The MVDR technique is summarized in Algorithm 1.

Algorithm 1 MVDR algorithm

- 1: **Input:** $x = \{x_i(t)\} = f(\alpha_i, \hat{\theta}_i), N, d, \lambda, K$ and $\mu \leftarrow$ step size
 - 2: Compute the weight vector w , Equation (18)
 - 3: Compute covariance matrix $\sigma(x, x)$, Equation (17)
 - 4: Compute the output array system, Equation (16)
 - 5: Minimize the output power, Equation (15), subject to $w \cdot a(\hat{\theta}) = 1$
 - 6: Compute spectrum function, Equation (19), spanning θ
-

4.2. MUSIC Algorithm

MUSIC is a high-resolution subspace DOA algorithm where an estimate $\sigma(x, x)$ of the covariance matrix is obtained and its eigenvectors decomposed into orthogonal signal and noise subspace [22]. The DOA is estimated from one of these subspaces. The noise in each channel is assumed uncorrelated. The algorithm searches through the set off all possible steering vectors to find the ones orthogonal to the noise subspace. The diagonal covariance matrix $\sigma(x, x)$ is given by Eq. (17). The covariance matrix is decomposed to

$$\sigma(x, x) = A(\hat{\theta}_i)\tilde{S}_i(t)A(\hat{\theta}_i)^H + \sigma^2 I = Q\Lambda Q^H, \tag{20}$$

where $A(\hat{\theta}_i) = [a_1(\hat{\theta}_1), a_2(\hat{\theta}_2), \dots, a_N(\hat{\theta}_I)]^T$ is a $M \times D$ array steering matrix, σ^2 the noise variance, I an identity matrix of size $M \times M$, and $\tilde{S}_i(t)$ the received signal with Q unitary and a diagonal matrix $\Lambda = \text{diag}\{\lambda_1, \lambda_2, \dots, \lambda_M\}$, of real eigenvalue ordered as $\lambda_1 \geq \lambda_2 \geq \dots \geq \lambda_M \geq 0$. The vector that is orthogonal to A is the eigenvector of R having the eigenvalues of Λ . The MUSIC spatial spectrum is defined by

$$P_{MUSIC}(\hat{\theta}) = \frac{1}{a^H(\hat{\theta})Q_n Q_n^H a(\hat{\theta})}, \tag{21}$$

where $a(\hat{\theta})$ is the steering vector corresponding to one of the incoming signals, and Q_n is the signal substance. The MUSIC technique is summarized in Algorithm 2.

Algorithm 2 MUSIC algorithm

- 1: **Input:** $x = \{x_i(t)\} = f(\alpha_i, \hat{\theta}_i), N, d, \lambda, K$
 - 2: Compute covariance matrix $\sigma(x, x)$, Equation (17)
 - 3: Decomposition $\sigma(x, x)$ into eigenvectors and eigenvalues in Equation (20)
 - 4: Rearrange the eigenvectors and eigenvalues into the signal subspace and noise subspace
 - 5: Compute the spectrum function (21) by spanning θ
 - 6: Determine the substantial peaks of $P_{MUSIC}(\theta)$ to acquire estimates of the angle of arrival
-

4.3. Proposed A-MUSIC Algorithm

In rain impacted mmW systems, the SNR is low leading to small signal intervals. The existing MVDR and MUSIC algorithms are adversely affected and need modifications. We propose an A-MUSIC algorithm that repeatedly reconstructs the covariance matrix to continuously obtain two noise and signal subspaces averaged over several iterations. The reconstructed covariance matrix $\hat{\sigma}(x, x)$ is given by

$$\hat{\sigma}(x, x) = \sigma(x, x) + J\sigma(x, x)^* J, \tag{22}$$

where J is MATLAB constructions given as $J = \text{fliplr}(\text{eye}(N))$ which returns columns flipped in the left-right direction, and N is the number of elements. The eigen decomposition on reconstructed covariance matrix $\hat{\sigma}(x, x)$ is

$$\hat{\sigma}(x, x) = \hat{Q}\hat{\Lambda}\hat{Q}^H = Q_{S1}\Lambda_{S1}Q_{S1}^H + Q_{N1}\Lambda_{N1}Q_{N1}^H, \tag{23}$$

where $\hat{\sigma}(x, x)$ is divided into signal subspace Q_S and noise subspace Q_N . Using low rank of matrix instead of full rank matrix $\hat{\sigma}(x, x)$ can be reconstructed into ω_x as

$$\omega_x = Q_{S2}\Lambda_{S2}Q_{S2}^H + Q_{N2}\Lambda_{N2}Q_{N2}^H. \quad (24)$$

The average signal subspace (Q_S), signal eigenvalue (Λ_S), noise subspace (Q_N), and the noise eigenvalue (Λ_N) are given by

$$\begin{aligned} Q_S &= \frac{Q_{S1} + Q_{S2}}{2}, \\ Q_N &= \frac{Q_{N1} + Q_{N2}}{2}, \\ \Lambda_S &= \frac{\Lambda_{S1} + \Lambda_{S2}}{2}, \\ \Lambda_N &= \frac{\Lambda_{N1} + \Lambda_{N2}}{2}. \end{aligned} \quad (25)$$

The A-MUSIC spectrum is then defined by

$$P_{(A-MUSIC)}(\hat{\theta}) = \frac{a^H(\hat{\theta}) \left[\frac{(\sigma(s,s))(\sigma(s,s))^H}{N} \right] a(\hat{\theta})}{a^H(\hat{\theta})\sigma(n,n)a(\hat{\theta})}, \quad (26)$$

where $\sigma(s, s) = Q_S\Lambda_S^{-1}Q_S^H$, and $\sigma(n, n) = Q_N\Lambda_N^{-1}Q_N^H$ are signal and noise subspace covariance matrix. The A-MUSIC technique is summarized in Algorithm 3.

Algorithm 3 Proposed A-MUSIC Algorithm

- 1: **Input:** $x = \{x_i(t)\} = f(\alpha_i, \hat{\theta}_i), N, d, \lambda, K$
 - 2: Compute the covariance matrix, Equation (20)
 - 3: Compute reconstructed covariance matrix $\hat{\sigma}(x, x)$, Equation (22)
 - 4: Compute the Eigen decomposition on reconstructed covariance matrix $\hat{\sigma}(x, x)$
 - 5: Compute reconstructed covariance matrix ω_x , for Equation (24)
 - 6: Compute the average signal subspace, noise subspace, signal eigenvalues, and the noise eigenvalue, $Q_S, Q_N, \Lambda_S, \Lambda_N$ Equation (25)
 - 7: Determine signal and noise subspace averaged covariance matrix $\sigma(s, s)$ and $\sigma(n, n)$
 - 8: Compute the spectrum function, Equation (26), spanning θ
-

5. PERFORMANCE MEASURES

The performance of the DOA estimation algorithms is evaluated in terms of spectrum functions, Equations (19), (21), and (26), Root Mean Square Error (RMSE), and signal to noise ratios. The RMSE is given by

$$RMSE = \sqrt{\frac{1}{K * N} \sum_{j=1}^K \sum_{i=1}^N (\tilde{\theta}_{ij} - \theta_i)^2}, \quad (27)$$

where K is the number of simulation trials; N is the number of elements; and the estimate of the i th angle of arrival in the j th trial is $\tilde{\theta}_{ij}$. The signal to noise ratio (SNR) is given by

$$SNR = 20 \log_{10} \left(\frac{x}{v} \right), \quad (28)$$

where x is the received signal strength in dB, and v is the noise strength in dB. The overall performance evaluation is done as in algorithm 4.

The complexity of MVDR and MUSIC algorithm has been derived as shown in Table 2 [23, 24]. For A-MUSIC, there are three major computational steps needed to estimate the DOA. The complexity

Algorithm 4 System Algorithm

-
- 1: **Input:** Required rainfall
 - 2: Compute expected rain rate, equation
 - 3: Compute the actual rain rate r from lognormal distribution with given mean
 - 4: **for** i number of antennas $< N_{\max}$
 - 5: Compute the rain attenuation α_r , total attenuation given
 - 6: A_T and the angle $\hat{\theta}_i$. find the angle deviation $\Delta\theta_i$ as shown
 - 7: in (13) and the mean μ_θ .
 - 8: Determine the received signal $x_i(t)$.
 - 9: **end for**
 - 10: Determine DOA, Algorithm 1, 2 and 3.
-

of the first step is the covariance function and reconstruction of the covariance matrix, $O(N^2K)$. The second step is the eigen-value decomposition operation, which has a complexity of $O(N^3)$. The third step is obtaining the spatial pseudo spectrum, which has a complexity of $O(J_\theta \cdot J_{\Delta\theta}(N+1)(N-K)/2)$, with J being the number of spectral points of the total angular field of view. Therefore, the total complexity of A-MUSIC is given by $O(N^2K + N^3) + O(J_\theta \cdot J_{\Delta\theta}(N+1)(N-K)/2)$.

Table 2. Computational complexity of DOA estimation algorithms.

DOA Algorithm	Computational Complexity
MVDR	$O(N^2K + N^3 + (2N^2 + 3N))$
MUSIC	$O(N^2K + N^3 + JN)$
A-MUSIC	$O(N^2K + N^3) + O(J_\theta \cdot J_{\Delta\theta}(N+1)(N-K)/2)$

6. RESULTS AND DISCUSSION

The performances of the general MVDR, MUSIC, and the proposed algorithm A-MUSIC are investigated and discussed in this section. The performance of the algorithms for different numbers of array elements, rain rates, and SNR is investigated. Unless otherwise specified for a particular result, the simulation parameters are as given in Table 3. The developed results are for a case where four signals impinge on the ULA sensors from the same signal source. The signal consists of the first direct path signal and the scaled and delayed replicas of the first signal representing multipath signals known priori. The background noise is modelled as a stationary Gaussian white random process.

The results of Figures 5(a)–(d) show the spatial output spectrum in dB's of the MVDR, MUSIC and the proposed A-MUSIC for different rain rates from zero to 20 mm/hr representing the following cases; no rain, widespread, shower and thunderstorm rain conditions with the number of elements $N = 5$ for 100 snapshots. Note that without rain the spectrum results for MVDR and MUSIC are similar to the ones in [25], respectively. From the results, the following can be observed; the accuracy of DOA estimation decreases with increasing rain rate, and the performance of the A-MUSIC is better than MUSIC followed by MVDR. This is because of the multiple averaging nature of A-MUSIC algorithm. It can also be observed that at a higher rain rate of 20 mm/hr MVDR and MUSIC fail to estimate the direction of arrival.

To analyse the performance of the DOA algorithms and the proposed method, a simulation was done for four neighbouring signals, and the results are tabulated in Table 4. The results depict the accuracy of the three DOA algorithms. There is a degradation in accuracy for the developed algorithm as the rain rate increases. From zero to 20 mm/hr the degradation of MVDR is 47%, for MUSIC is 33%, and for A-MUSIC is 3.3% at reference point -20 dB.

Table 3. Simulation parameters for MVDR, MUSIC and A-MUSIC algorithm.

Simulation Parameters	Values
Input θ	$[0^0, 10^0, 35^0, 60^0]$
Number of elements	$N = 5, N = 15$
Spacing difference	$d = 0.5\lambda$
Signal-to-noise ratio	$SNR = 20$ dB
Snapshots	$K = 100$
Rain rate in (mm/h)	$[0, 2.5, 6, 12, 20]$
a at f (GHz)	0.7103
k at f (GHz)	1.16995
$\Delta\theta_{\min}, \Delta\theta_{\max}$	$[0^0 - 65^0]$

Table 4. Spectrum performance for actual DOA = $[0^0, 10^0, 35^0, 60^0]$.

Figure 5(a)	Estimated DOA	Error %
MVDR	$0.0201^0, 9.9^0, 35.01^0, 59.8^0$	3.372
MUSIC	$0.02^0, 10.001^0, 35.02^0, 60^0$	2.067
A-MUSIC	$0^0, 10^0, 35^0, 60^0$	0
Figure 5(b)	Estimated DOA	Error %
MVDR	$-0.032^0, 9.8^0, 34.0^0, 58.8^0$	10.057
MUSIC	$1.2^0, 10.5^0, 34.78^0, 60.1^0$	17.796
A-MUSIC	$0.001^0, 10^0, 35^0, 60^0$	0.1
Figure 5(c)	Estimated DOA	Error %
MVDR	$0.22^0, 9.5^0, 34.76^0, 62^0$	31.018
MUSIC	$0.1^0, 10.3^0, 34.8^0, 61.1^0$	15.404
A-MUSIC	$0.001^0, 10.002^0, 35.03^0, 60.01^0$	0.2217
Figure 5(d)	Estimated DOA	Error %
MVDR	$-0.32^0, 11.1^0, 35.7^0, 63.2^0$	50.33
MUSIC	$0.2^0, 10.2^0, 36.0^0, 63.0^0$	29.86
A-MUSIC	$0.01^0, 10.2^0, 35.1^0, 60.01^0$	3.303

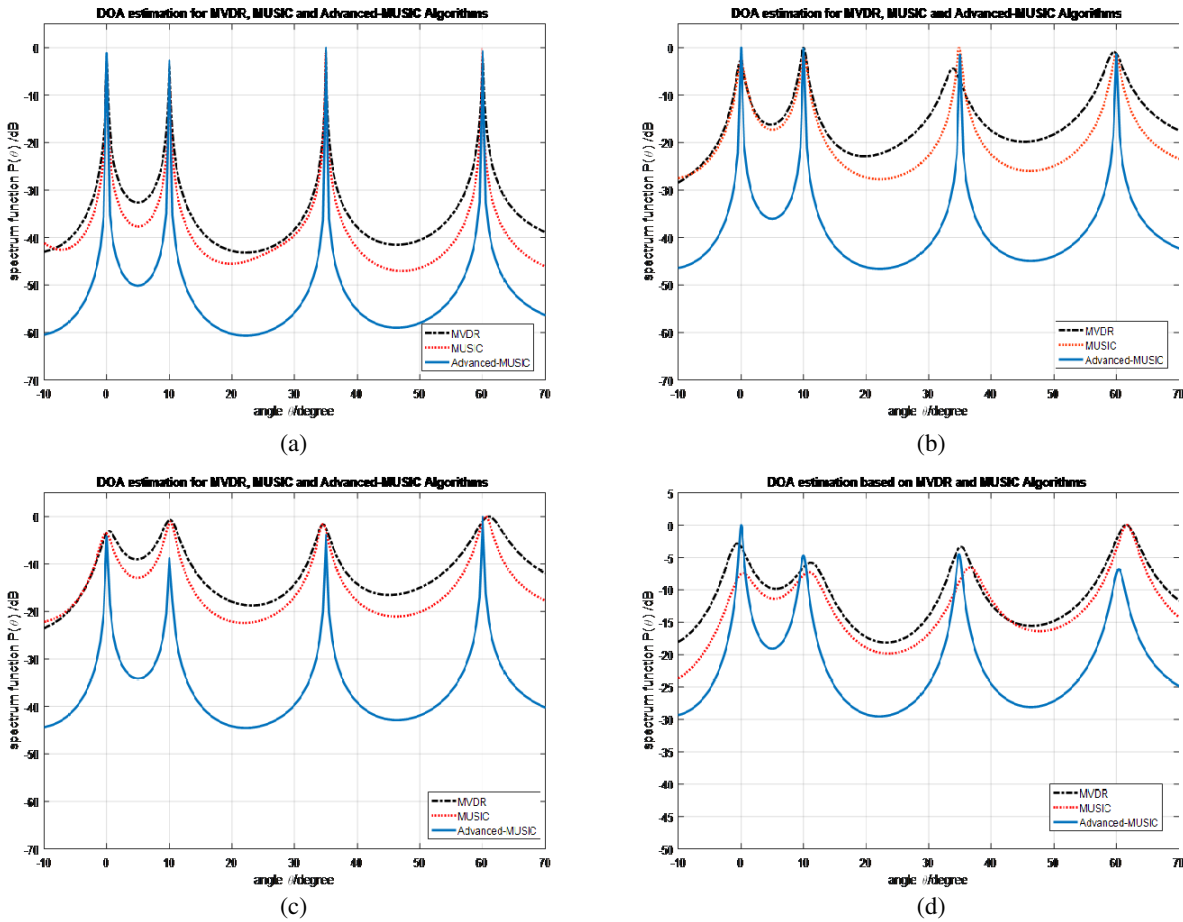


Figure 5. DOA estimation attenuation for $N = 5$ with various rainfall rates. (a) DOA estimation attenuation with rain rate $r = 0$ mm/hr for $N = 5$. (b) DOA estimation attenuation at drizzle rain rate $r = 2$ mm/hr for $N = 5$. (c) DOA estimation attenuation at widespread rain rate $r = 8$ mm/hr for $N = 5$. (d) DOA estimation attenuation at shower rain rate $r = 20$ mm/hr for $N = 5$.

Similarly, the results of Figures 6(a)–(d) show the spatial output power spectrum in dB’s of the three algorithms discussed in Section 4 for different rain rates representing no rain, widespread, shower and thunderstorm rain conditions. However, the number of elements $N = 15$ for 100 snapshots. Note that without rain the spectrum results for MVDR and MUSIC are similar to the ones in [26, 27], respectively. The results reinforce the notion that the accuracy of DOA estimation decreases with increasing rain rate, and the performance of the A-MUSIC is better than MUSIC followed by MVDR.

The results of estimated DOAs are tabulated in Table 5. Similarly, the results depict the accuracy of the three DOA algorithms. There is a degradation in accuracy for the developed algorithm as the rain rate increases. From zero to 20 mm/hr, the degradation of MVDR is 38%, for MUSIC is 23%, and for A-MUSIC is 1.23% at reference point -20 dB.

For different numbers of antennas, comparison of the results in Figures 5(a)–(d) for $N = 5$ and Figures 6(a)–(d) for $N = 15$ is done. We observe that DOA estimation improves with increasing the number of antenna elements. At the -40 dB reference point, we observe that the width of the spectrum function is wide, leading to high error estimation of the angle of arrival.

The results of Figure 7 represent the RMSE value vs rain rate at a different angle of arrival $[20^\circ, 40^\circ, 50^\circ]$ for two different reference spectrum function levels -20 dB and -40 dB with $N = 10$. As expected, the RMSE increases with an increase in rain rate. It is also higher at -40 dB than -20 dB. The performance order of the algorithms is MVDR, MUSIC, and A-MUSIC. Similarly, the results of Figures 8(a)–(c) represent the RMSE error comparison for different rain conditions albeit at

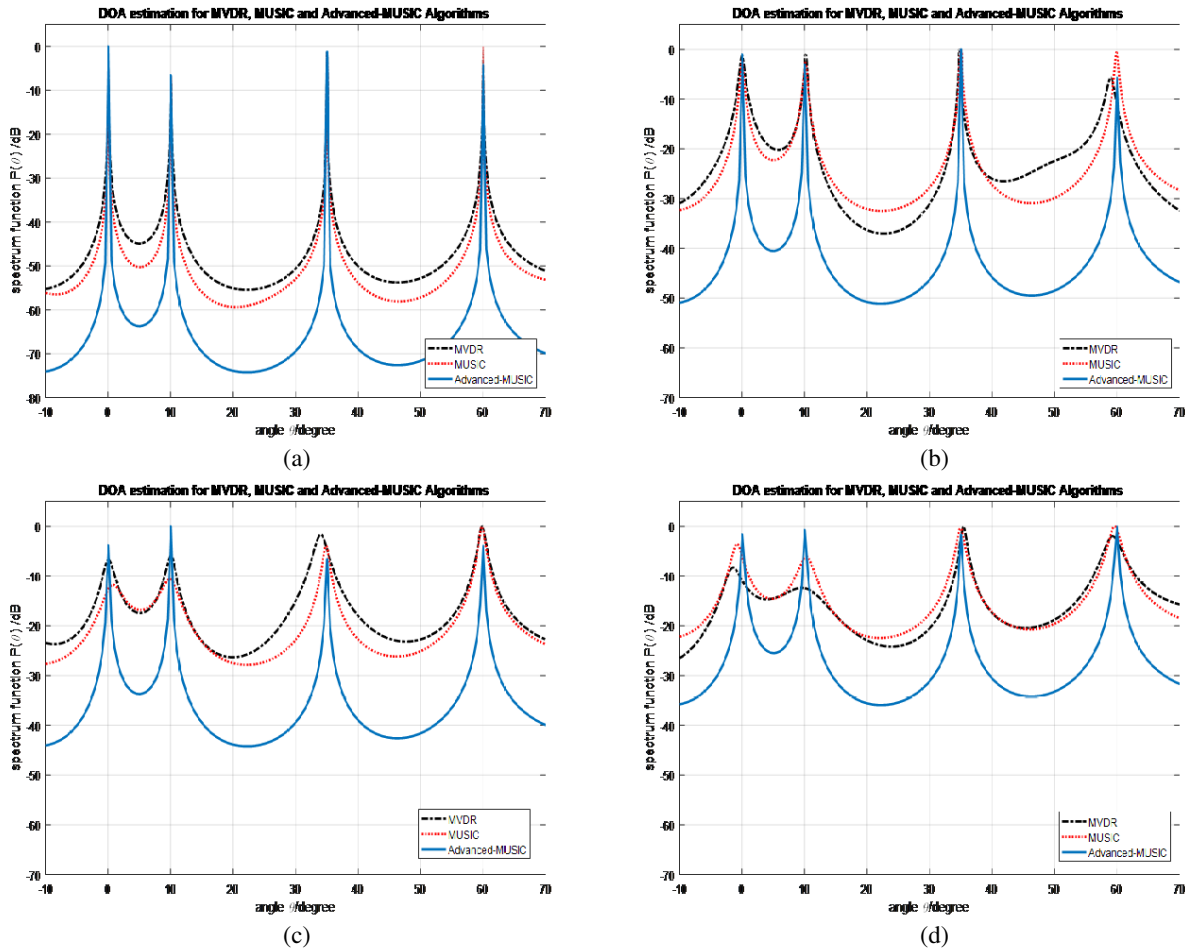


Figure 6. DOA estimation attenuation for $N = 15$ with various rainfall rates. (a) DOA attenuation with rain rate $r = 0$ mm/hr for $N = 15$. (b) DOA attenuation in light rain rate of $r = 2$ mm/hr for $N = 15$. (c) DOA attenuation in moderate rain rate of $r = 8$ mm/hr for $N = 15$. (d) DOA attenuation in heavy rain rate of $r = 20$ mm/hr for $N = 15$.

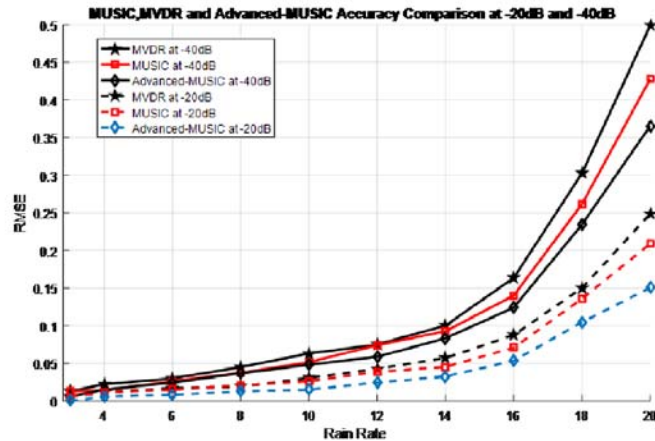


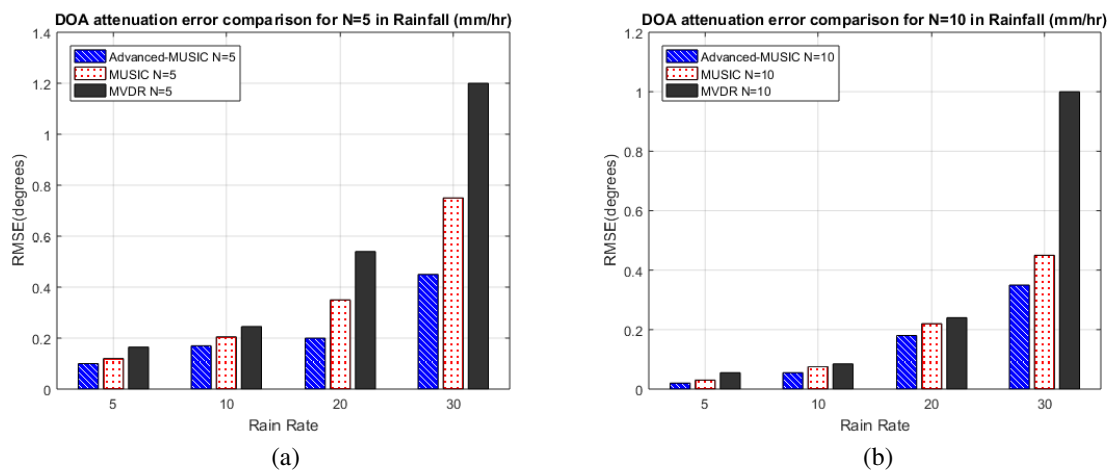
Figure 7. MUSIC, MVDR and A-MUSIC accuracy comparison at -20 dB and -40 dB with $\text{DOA} = [20^\circ, 40^\circ, 50^\circ]$.

Table 5. Spectrum performance for actual DOA = $[0^0, 10^0, 35^0, 60^0]$.

Figure 6(a)	Estimated DOA	Error %
MVDR	$0^0, 10.001^0, 35.02^0, 60.01^0$	0.5977
MUSIC	$0.002^0, 10.01^0, 35.01^0, 60.02^0$	0.3623
A-MUSIC	$0^0, 10^0, 35^0, 60^0$	0
Figure 6(b)	Estimated DOA	Error %
MVDR	$0.2^0, 10.1^0, 33.7^0, 59.6^0$	25.381
MUSIC	$0.01^0, 10.2^0, 34.7^0, 60.1^0$	4.024
A-MUSIC	$0.001^0, 10.01^0, 35.01^0, 60^0$	0.2286
Figure 6(c)	Estimated DOA	Error %
MVDR	$0.23^0, 9.6^0, 35.3^0, 57.5^0$	32.024
MUSIC	$0.1^0, 10.2^0, 35.01^0, 60.01^0$	12.0453
A-MUSIC	$0.01^0, 10^0, 35^0, 60^0$	1.0
Figure 6(d)	Estimated DOA	Error %
MVDR	$-3^0, 9.5^0, 34.5^0, 58.5^0$	38.929
MUSIC	$-2^0, 10.2^0, 35.1^0, 59.5^0$	23.00
A-MUSIC	$0.002^0, 9.9^0, 35.01^0, 60^0$	1.2286

variable antenna elements $N = 5, N = 10,$ and $N = 20$ for $SNR = 20$ dB. The RMSE increases with increase in rainfall, and the proposed A-MUSIC performs better than the other models due to repeatedly reconstruction of the covariance matrix to obtain two noise and signal subspaces continuously that are averaged for several iterations. An additional deduction from the result is that the RMSE errors decrease with the increase in antenna elements.

To reiterate the deduction from Figures 8(a)–(c), Figure 9 presents the results of the RMSE error vs



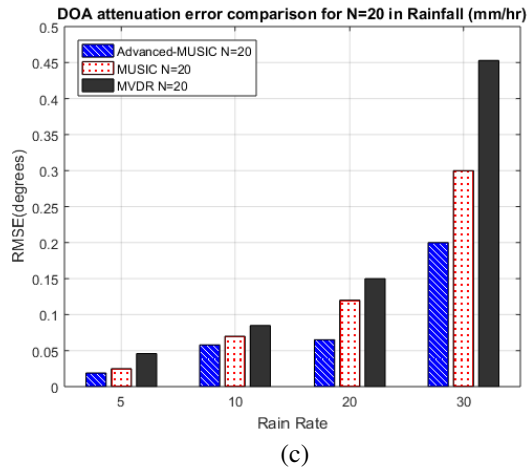


Figure 8. DOA estimation attenuation error comparison. (a) DOA estimation attenuation error comparison for $N = 5$. (b) DOA estimation attenuation error comparison for $N = 10$. (c) DOA estimation attenuation error comparison for $N = 20$.

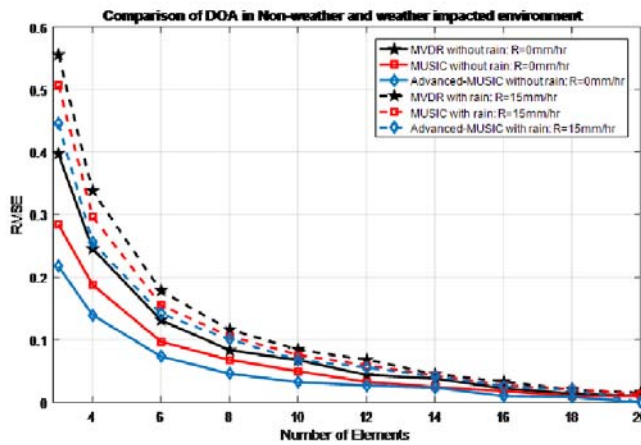


Figure 9. Comparison of DOA estimation algorithms in non-weather and weather impacted environment.

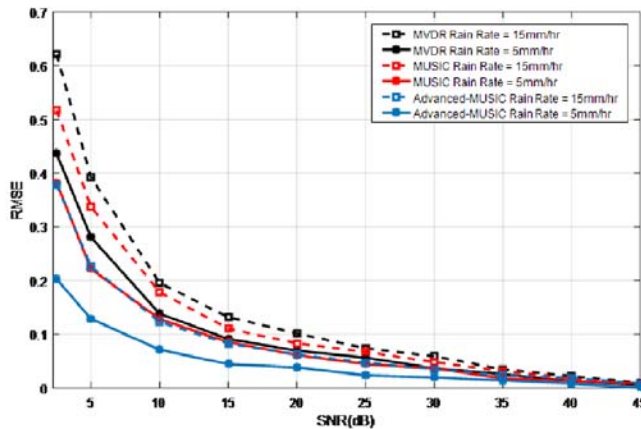


Figure 10. Error comparison in various rain rates vs SNR.

the number of elements for no rain and the rate of 15 mm/hr. It can be observed that as the number of elements increases the RMSE decreases. Still the proposed A-MUSIC outperforms MVDR and MUSIC algorithms in terms of error comparison. We conclude that the statistical channel model proposed in this paper is highly recommended in both rainfall and non-rainfall regions due to its excellent performance.

To further investigate the performance of the system, the DOA estimation algorithms are tested at different rain rates leading to different SNR conditions and results presented in Figure 10 for $N = 10$. As expected, the RMSE decreases with an increase in the values SNR, and A-MUSIC outperforms MVDR and MUSIC making it highly recommended in estimation of DOA in both normal and rainfall environments.

Figure 11 shows the performance comparison in rainfall for various numbers of snapshots at $SNR = 20$ dB, $r = 20$ mm/hr, and $N = 5$. As expected, the RMSE decreases as we increase the number of trials from 100 to 500. Therefore, increasing number of simulation trials can improve the performance of the algorithms. It can be intuitively observed that the proposed A-MUSIC surpasses the MVDR and classical MUSIC estimator over the range of the number of snapshots that we simulated.

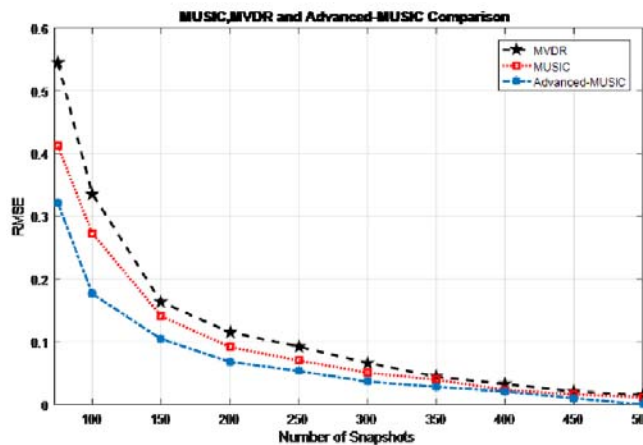


Figure 11. Error comparison in RMSE vs number of snapshots.

7. CONCLUSION

This work has investigated the performance of the existing DOA algorithms, MVDR, and MUSIC compared with our proposed A-MUSIC on a weather-impacted network. The investigation is conducted for conditions of no rain, widespread, shower and thunderstorm rainfall. The deduction from the investigation indicates that the algorithms performance accuracy degrades by up to 43% and 28% for MVDR and MUSIC, respectively, from no rain condition to thunderstorm rainfall condition with MUSIC performing better than MVDR. The RMSE performance of the algorithms is shown to decrease by increasing the values of SNR and number of antenna elements. The work develops an A-MUSIC algorithm for the weather impacted conditions. The performance of the developed A-MUSIC is superior to the existing algorithm in terms of accuracy and RMSE parameters. The performance accuracy degrades by up to 2.3% from no rain condition to thunderstorm rainfall condition. However, its complexity is higher than the other algorithms. This work opens further investigation into the performance of DOA algorithms in weather impacted environment and the need for redesign of the existing algorithms. The accuracy of the investigation could be validated further by the derivation of the Cramer-Rao lower bounds and other statistical measures.

REFERENCES

1. Tsoulos, G. V., "Smart antennas for mobile communication systems: Benefits and challenges," *IEE Electron. Commun. Eng. Journal*, Vol. 11, No. 2, 84-94, April 1999.

2. Lavate, T. V., V. K. Kokate, and A. M. Sakpal, "Performance analysis of MUSIC and ESPRIT DOA estimation algorithms for adaptive array smart antenna in mobile communication," *Proc. of IEEE, Second Int. Conf. Computer and Network Technology*, 308–311, 2010.
3. Shaukat, S. F., H. Mukhtar, R. Farooq, H. U. Saeed, and Z. Saleem, "Sequential studies of beamforming algorithms for smart antenna systems," *World Applied Sciences Journal*, Vol. 6, No. 6, 754–758, 2009.
4. Balanis, C., *Antenna Theory: Analysis and Design*, 3rd Edition, John Wiley and Sons, Hoboken, New Jersey, 2005.
5. Leon De, F. A. and S. J. J Marciano, "Application of MUSIC, ESPRIT and SAGE algorithms for narrowband signal detection and localization," *TENCON, IEEE Reg. 10 Conf.*, 1–4, 2006.
6. Qian, C., H. Lei, and H. C. So, "Computationally efficient ESPRIT algorithm for direction-of-arrival estimation based on Nyström method," *Signal Processing*, Vol. 94, 74–80, 2014.
7. Xu, C. and J. Krolik, "Space-delay adaptive processing for MIMO RF indoor motion mapping," *IEEE. Int. Conf. on Acoustics, Speech and Signal Processing (ICASSP)*, 2349–2353, Brisbane, QLD, April 2015.
8. Dhope, T., D. Simunic, and M. Djurek, "Application of DOA estimation algorithms in smart antenna systems," *Studies in Informatics and Control*, Vol. 19, No. 4, 445–452, December 2010.
9. Schmidt, R., "Multiple emitter location and signal parameter estimation," *IEEE Transactions on Antennas and Propagation*, Vol. 34, No. 3, 276–280, 1986.
10. Roy, R. and T. Kailath, "ESPRIT—a subspace rotational approach to estimation of parameters of cissoids in noise," *IEEE Transactions on Acoustics, Speech, and Signal Processing*, Vol. 34, No. 10, 1340–1342, 1986.
11. Zhang, Y., P. Wang, and Goldsmith, "Rainfall effect on the performance of millimeter-wave MIMO systems," *IEEE Transactions on Wireless Communications*, Vol. 14, No. 9, 4857–4866, September 2015.
12. Pi, Z. and F. Khan, "An Introduction to millimeter-wave mobile broadband systems," *IEEE Commun. Mag.*, Vol. 49, No. 6, 101–107, June 2011.
13. Ishimaru, A., *Wave Propagation and Scattering in Random Media*, IEEE Press, Piscataway, NJ, USA, 1978.
14. Ishimaru, A., S. Jaruwatanadilok, and Y. Kuga, "Multiple scattering effects on the radar cross section (RCS) of objects in a random medium including backscattering enhancement and shower curtain effects," *Waves Random Media*, Vol. 14, 499–511, 2004.
15. Agber, J. U. and J. M. Akura, "A high-performance model for rainfall effect on radio signals," *Journal of Information Engineering and Applications*, Vol. 3, No. 7, 1–12, 2013.
16. Calla, O. and J. Purohit, "Study of effect of rain and dust on propagation of radio waves at millimeter wavelength," *International Centre for Radio Science*, 1–4, 'OM NIWAS'A-23 Shastri Nagar Jodhpur, January 1990.
17. Alonge, A. A. and T. J. Afullo, "Fractal analysis of rainfall event duration for microwave and millimetre networks: Rain queueing theory approach," *IET Microwaves, Antennas and Propagation*, Vol. 9, No. 4, 291–300, 2015.
18. Kedem, B. and L. S. Chiu, "On the lognormality of rain rate," *Proceedings of the National Academy of Sciences*, Vol. 84, No. 4, 901–905, 1987.
19. Cho, H. K., K. P. Bowman, and G. R. North, "A comparison of gamma and lognormal distributions for characterizing satellite rain rates from the tropical rainfall measuring mission," *Journal of Applied Meteorology*, Vol. 43, No. 11, 1586–1597, 2004.
20. I.T.U. Radiowave Propagation Series, "Specific attenuation model for rain for use in prediction methods," *Rec. P.838-3, ITU-R*, Geneva, Switzerland, 2005.
21. Oh, D., Y. Ju, and J. Lee, "An improved MVDR-like TOA estimation without EVD for high-resolution ranging system," *IEEE Communications Letters*, Vol. 18, No. 5, 753–756, May 2014.
22. El Gonnouni, A., M. Martinez-Ramon, J. L. Rojo-Alvarez, G. Camps-Valls, A. R. Figueiras-Vidal, and C. G. Christodoulou, "A support vector machine MUSIC algorithm," *IEEE Transactions on*

Antennas and Propagation, Vol. 60, No. 10, 4901–4910, October 2012.

23. Balakrishnan, S. and L. T. Ong, “GNU radio based digital beamforming system: BER and computational performance analysis,” *Proc. of the 2015 23rd European Signal Processing Conference (EUSIPCO)*, 1596–1600, Nice, France, August 31–September 4, 2015.
24. Stoeckle, C., J. Munir, A. Mezghani, and J. A. Nossek, “DOA estimation performance and computational complexity of subspace- and compressed sensing-based methods,” *Proc. in WSA 2015 19th International ITG Workshop on Smart Antennas*, 1–6, March 2015.
25. Bhaumik, B., “Performance analysis of MUSIC algorithm for DOA estimation,” *International Research Journal of Engineering and Technology (IRJET)*, Vol. 4, 1667–1670, February 2017.
26. Aboul-Seoud, A. K., A. K. Mahmoud, A. Hafez, and A. Gaballa, “Minimum variance variable constrain DOA algorithm,” *PIERS Proceedings*, 798–803, Guangzhou, China, August 25–28, 2014.
27. Kokare, R. G. and V. S. Hendre, “Estimation of direction of arrival using music and esprit algorithm for smart antenna,” *International Journal of Control Theory and Applications*, Vol. 10, No. 38, 2017.